Woods-Saxon-Gaussian potential and alpha-cluster structures of alpha + closed shell nuclei *

Dong Bai(柏栋)[1;1)] Zhongzhou Ren(任中洲)[2;2)]

[1] School of Physics, Nanjing University, Nanjing 210093, China
[2] School of Physics Science and Engineering, Tongji University, Shanghai 200092, China

Abstract: The Woods-Saxon-Gaussian (WSG) potential is proposed as a new phenomenological potential to systematically describe the level scheme, electromagnetic transitions, and alpha-decay half-lives of the alpha-cluster structures in various alpha + closed shell nuclei. It modifies the original Woods–Saxon (WS) potential with a shifted Gaussian factor centered at the nuclear surface. The free parameters in the WSG potential are determined by reproducing the correct level scheme of ^{212}Po=^{208}Pb+α. It is found that the resulting WSG potential matches the M3Y double-folding potential at the surface region and makes corrections to the inner part of the cluster-core potential. It was also determined that the WSG potential, with nearly identical parameters to that of ^{212}Po (except for a rescaled radius), could also be used to describe alpha-cluster structures in ^{20}Ne=^{16}O+α and ^{44}Ti=^{40}Ca+α. In all three cases, the calculated values of the level schemes, electromagnetic transitions, and alpha-decay half-lives agree with the experimental data, which indicates that the WSG potential could indeed capture many important features of the alpha-cluster structures in alpha + closed shell nuclei. This study is a useful complement to the existing cluster-core potentials in literature. The Gaussian form factor centered at the nuclear surface might also help to improve our understanding of the alpha-cluster formation, which occurs in the same general region.

Keywords: alpha cluster, alpha decay, cluster-core potential

PACS: 21.60.Gx , 23.60.+e **DOI:** 10.1088/1674-1137/42/12/124102

1 Introduction

Alpha clusters play a crucial role in nuclear physics. Alpha clustering in light nuclei was proposed in the 1930s [1] and has been studied intensively since then, especially after the proposal of the existence of alpha-particle condensates in Hoyle and Hoyle-like states in 2001 [2]. See, e.g., Ref. [3] for a recent discussion on the impact of repulsive four-body interactions of alpha particles on the physical properties of alpha-particle condensates. Inspired by Ref. [2], nonlocalized clustering is proposed as a new concept in cluster physics, and an exemplifying calculation is performed for the inversion-doublet band of ^{20}Ne [4]. Alpha clustering could also exist in heavy/superheavy nuclei, as suggested by the observation of alpha decay in these nuclei. The theoretical explanation of alpha decay dates back to the celebrated papers by Gamow, Gurney, and Condon [5, 6]. Currently, numerous phenomenological models have been proposed to explain the observed alpha-decay and spectroscopic data, in which the parent nucleus is modeled as a binary system consisting of a tightly bound alpha cluster and the remaining core nucleus (see, e.g., Ref. [7–17]). The relative motion between these two constituents then gives rise to various properties of the parent nuclei. For later convenience, we shall refer to these phenomenological models as binary cluster models (BCMs). It is interesting to note that some of the BCMs could describe alpha clustering not only in heavy nuclei, but also in light and medium-mass nuclei such as ^{20}Ne and ^{44}Ti [9]. In Ref. [18–24], a new phenomenological model called the density-dependent cluster model was proposed and developed, which takes into consideration the impact of nuclear density distributions and facilitates a better description of experimental alpha-decay data . Microscopic descriptions of alpha decay and alpha clustering in heavy nuclei were also pursued. One of the milestones of the significant work done by Ref. [25] is that it results in a satisfying description of ground-state alpha decay in ^{212}Po based on the cluster-configuration shell model. For

Received 11 July 2018, Published online 22 October 2018

∗ Supported by the National Natural Science Foundation of China (11535004, 11761161001, 11375086, 11120101005, 11175085, 11235001), the National Key R&D Program of China (2018YFA0404403, 2016YFE0129300) and the Science and Technology Development Fund of Macau (008/2017/AFJ)

1) E-mail: dbai@itp.ac.cn

2) E-mail: Corresponding Author: zren@tongji.edu.cn

more recent works on microscopic descriptions of ^{212}Po, see, e.g., Ref. [26–30]. We also recommend Ref. [31] for a comprehensive introduction to alpha clustering in heavy nuclei.

The successful application of the BCM is critically dependent on the choice of the cluster-core nuclear potential. The simplest choice might be the square-well potential [7]. More realistic choices for the phenomenological potential include the double-folding potential based on, e.g., the M3Y nucleon-nucleon interaction [18], the so-called Cosh potential obtained by fitting the double-folding potential [8], the Woods–Saxon (WS) potential inspired by the shell model [19], the WS+WS^3 potential [9, 12], a new local potential proposed in Ref. [32], etc. By utilizing the Bohr–Sommerfeld–Wildermuth quantization condition [33] to mimic the Pauli blocking effects, all these potentials can readily reproduce satisfactory results for alpha-decay half-lives for heavy and superheavy alpha-emitters. However, further studies indicate that the M3Y potential, the Cosh potential, and the WS potential fail to explain the observed energy spectrum of ^{212}Po=^{208}Pb+α, which is a canonical example of alpha + closed shell nuclei, and typically yields inverted level schemes [9, 10]. As such, the WS+WS^3 potential is essentially the default approach for spectroscopic studies of alpha-cluster structures of ^{212}Po in the literature . In this work, we aim to propose a new phenomenological potential between the cluster and core nuclei. ^{212}Po is used as a benchmark nucleus to determine the free parameters of the potential. Later, these parameters with the radii rescaled are shown to describe alpha clusters in light and medium-weight nuclei as well.

2 Formalism

In general, a cluster-core nuclear potential, which aims to provide a satisfactory description of alpha decay of ^{212}Po should be in agreement with the WS potential or the M3Y potential at the surface region. However, as previously noted, the WS potential alone fails to provide the correct level scheme. Also, it is well-known that the alpha-cluster formation process actually occurs in the vicinity of the nuclear surface [31]. Within such a framework, the alpha cluster loses its identity and merges with the core nucleus when moving towards the center of the core nucleus. A satisfactory phenomenological potential might be able to provide hints regarding the details of this process . Considering these factors, we introduce the following general form for the cluster-core nuclear potential,

$$V_{\rm N}(r)=-\frac{V_0 f(r)}{1+\exp[(r-R)/a]}, \tag{1}$$

where $f(r)$ is the form factor that encodes corrections to the inner part of the WS potential. Microscopically, this nontrivial form factor $f(r)$ might be related to the alpha-cluster formation around the nuclear surface and other quantum mechanical effects. The form factor $f(r)$ could be investigated on a Gaussian basis,

$$f(r)=1+\sum_i \alpha_i \exp[-\beta_i (r-R_i)^2], \tag{2}$$

as a result of the over-completeness of the Gaussian basis [34]. In this work, we only take the leading-order correction for simplicity,

$$V_{\rm N}(r)=-\frac{V_0}{1+\exp[(r-R)/a]}\{1+\alpha\exp[-\beta(r-R)^2]\}. \tag{3}$$

In this case, it is crucial to note that the same R in the WS potential is used as the R_1 in the Gaussian form factor. In other words, we plan to modify the WS potential with a Gaussian form factor center at the nuclear surface. This is by no means trivial. Generally, an arbitrary function $f(r)$ does not allow such an identification. As shown later, this choice is able to provide reasonable descriptions for alpha-cluster structures in alpha + closed shell nuclei. It is natural to guess that the underlying physics is related to the previously mentioned alpha-cluster formation process. In fact, the proposal to use additional Gaussian alpha-like components was first implemented within the cluster-configuration shell model by Ref. [25] and later in Ref. [28]. In the following, we shall call Eq. (3) as the Woods–Saxon–Gaussian (WSG) potential. We intend to use this model to provide a systematic treatment of various nuclear structural and alpha-decay properties. V_0, R, a, α, and β are five free parameters that are determined by reproducing specific experimental observations. The usefulness of the WSG potential will be justified by a comparison of theoretical calculations with experimental data for ^{212}Po. The WSG potential in Eq. (3) can certainly be further improved by including more Gaussian terms in the braces.

Given values for the free parameters, the WSG potential can be used to calculated the spectrum of ^{212}Po. In this instance, we use the Bohr–Sommerfeld–Wildermuth quantization condition:

$$\int_{r_1}^{r_2}\sqrt{\frac{2\mu}{\hbar}[E_L-V(r)]}{\rm d}r=(G-L+1)\frac{\pi}{2}, \tag{4}$$

$$V(r)=V_{\rm N}(r)+V_{\rm C}(r)+V_L(r), \tag{5}$$

to calculate the spectrum. $V_{\rm N}(r)$ is the WSG potential given by Eq. (3). $V_{\rm C}(r)$ is the Coulomb potential defined as:

$$V_{\rm C}(r)=\begin{cases}\dfrac{Z_c Z_\alpha e^2}{r}, & r\geqslant R,\\ \dfrac{Z_c Z_\alpha e^2}{2R}\left[3-\left(\dfrac{r}{R}\right)^2\right], & r<R.\end{cases} \tag{6}$$

$V_L(r)$ is the centrifugal potential in the Langer approxi-

mation

$$V_L(r)=\frac{\hbar^2}{2\mu r^2}\left(L+\frac{1}{2}\right)^2. \quad (7)$$

The quantum number G is chosen to be $G=18$ for ^{212}Po [9, 10]. r_1 and r_2 are the inner classical turning points. μ is the reduced mass of the alpha cluster. E_L is the energy of the state with the orbital angular momentum L.

The WSG potential can also be used to study alpha decays and electromagnetic transitions of ^{212}Po. The alpha-decay width is estimated by using the two-potential approach [35, 36],

$$\begin{aligned}&\Gamma_\alpha=P_\alpha F\frac{\hbar^2}{4\mu}\exp\left[-2\int_{r_2}^{r_3}\mathrm{d}rk(r)\right],\\&k(r)=\sqrt{\frac{2\mu}{\hbar^2}|E_L^{\rm Exp}-V(r)|},\\&F\int_{r_1}^{r_2}\mathrm{d}r\frac{1}{k(r)}\cos^2\left(\int_{r_1}^{r}\mathrm{d}r'k(r')-\frac{\pi}{4}\right)=1, \quad (8)\end{aligned}$$

where P_α is the preformation probability of the alpha cluster in ^{212}Po and r_3 is the outer classical turning points of the Coulomb barrier. The reduced quadrupole transition strength from an initial state of the angular momentum L to a final state of the angular momentum $L-2$ can be calculated by [10]:

$$\begin{aligned}B(\mathrm{E2};L\to L-2)=&\frac{15\beta_2^2}{8\pi}\frac{L(L-1)}{(2L+1)(2L-1)}\\&\times\left|\int_0^\infty\psi_{L-2}(r)^*r^2\psi_L(r)\mathrm{d}r\right|^2, \quad (9)\\\beta_2=&e\frac{Z_cA_\alpha^2+Z_\alpha A_c^2}{(A_c+A_\alpha)^2}, \quad (10)\end{aligned}$$

where $\psi_L(r)$ is the radial wave function of the angular momentum L.

3 Numerical results

In the remainder of this article, we shall first apply the WSG potential to study alpha-cluster structures in ^{212}Po. The free parameters of the WSG potential are determined by minimizing $\chi^2=\sum_L(E_L^{\rm exp}-E_L^{\rm present})^2$ and simultaneously reproducing the correct level scheme of ^{212}Po. Experimentally, the energy of the 16^+ state has not been measured as yet, but it is reasonable to assume that $E_{14}^{\rm present}<E_{18}^{\rm present}<E_{16}^{\rm present}$, which is able to hinder the electromagnetic decay of the 18^+ state. As a result, the 18^+ state mainly decays via alpha decay, and the decay rate is then strongly suppressed by the large centrifugal barrier. This could provide a natural explanation of the isomeric character of the 18^+ state and its observed decaying branching ratio which is monopolized by alpha decay ($\sim 100\%$). Such an assumption is also consistent with previous studies, e.g., Ref. [12]. After a moderate amount of trial and error, the free parameters in the WSG potential are chosen as follows:

$$\begin{aligned}&V_0=203.3\ \mathrm{MeV},\quad a=0.73\ \mathrm{fm},\quad R=6.73\ \mathrm{fm},\\&\alpha=-0.478,\quad \beta=0.054\ \mathrm{fm}^{-2}. \quad (11)\end{aligned}$$

In Fig. 1, we compare the WSG potential with the M3Y potential obtained by double-folding the M3Y nucleon-nucleon interactions. The technical details for the M3Y double-folding potential calculation are presented in Appendix A. The WSG potential was determined to approximately match the M3Y potential in the surface region with $r>6$ fm.

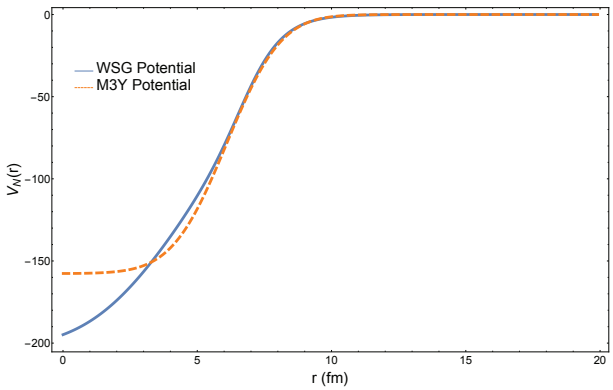

Fig. 1. (color online) The WSG potential with parameters given by Eq. (11) and the M3Y potential with the renormalization factor $\lambda=0.51$. The WSG potential approximately matches the M3Y potential in the surface region with $r>6$ fm.

Table 1. The experimental level scheme of ^{212}Po and the theoretical calculations obtained with the WSG potential with the parameters given by Eq. (11). The experimental values are taken from Ref. [26, 27].

J^π	$E_L^{\rm exp}$/MeV	$E_L^{\rm present}$/MeV
0^+	0.000	0.076
2^+	0.727	0.255
4^+	1.132	0.596
6^+	1.355	1.050
8^+	1.476	1.581
10^+	1.834	2.141
12^+	2.702	2.676
14^+	2.885	3.108
16^+	–	3.328
18^+	2.921	3.152

In Table 1, we tabulate the experimental level scheme of ^{212}Po based on theoretical results obtained using the WSG potential with the parameters given by Eq. (11). The reduced transition strengths $B(\mathrm{E2}\downarrow)$ obtained by using the WSG potential are tabulated in Table 2. All values therein are given in Weisskopf units (W.u.). The theoretical values agree with the experimental data within a

factor of 2, and reproduce the observed trend with good agreement. The alpha-decay half-lives $T^{\alpha}_{1/2}=\hbar\ln 2/\Gamma_{\alpha}$ are calculated using Eq. (8), and are tabulated in Table 3. The preformation factor is taken to be P_{α}=0.6 to achieve better agreement with experimental data. It was determined that most of the theoretical values are within a factor of 2 compared to the experimental values.

Table 2. Theoretical values of the reduced quadrupole transition strengths of ^{212}Po obtained with the WSG potential with the parameters given by Eq. (11). All values are in the unit of the so-called Weisskopf unit (W.u.) given by 1 W.u. $=\frac{0.746}{4\pi}A^{4/3}$ e^2·fm^4. Here, $A=A_{\alpha}+A_c=212$ is the mass number of ^{212}Po, and e is the elementary charge. The experimental values are taken from Ref. [26, 27].

transition	B(E2↓)$_{\rm exp}$/(W.u.)	B(E2↓)$_{\rm present}$/(W.u.)
$2^+\to0^+$	–	4.4
$4^+\to2^+$	–	6.1
$6^+\to4^+$	3.9±1.1	6.3
$8^+\to6^+$	2.3±0.1	5.9
$10^+\to8^+$	2.2±0.6	5.2
$12^+\to10^+$	–	4.4
$14^+\to12^+$	–	3.4
$16^+\to14^+$	–	2.3

Given the above results on ^{212}Po, we further apply the WSG potential to light nuclei ^{20}Ne = ^{16}O+α and ^{44}Ti = ^{40}Ca+α. We take the same parameter set given by Eq. (11), except R=3.25 fm for ^{20}Ne and R=4.61 fm for ^{44}Ti, which are determined by minimizing χ^2 for the level schemes of ^{20}Ne and ^{44}Ti respectively. The quantum number G is taken to be G=8 for ^{20}Ne and G=12 for ^{44}Ti. The calculated values are listed in Tables 4 and 5, which also agree with the experimental values. In particular, the calculated values for the electromagnetic transition strengths are in agreement with the experimental values within a factor of 1.1∼1.3 for ^{20}Ne and 1∼1.7 for ^{44}Ti.

Table 3. Alpha-decay half-lives for different states of ^{212}Po. $T^{\alpha,\rm exp}_{1/2}$ and $T^{\alpha,\rm present}_{1/2}$ denote the experimental and theoretical values of the alpha-decay half-lives [26, 27]. The theoretical values are calculated using the performance factor P_{α}=0.6.

J^{π}	$T^{\alpha,\rm exp}_{1/2}$/ns	$T^{\alpha,\rm present}_{1/2}$/ns
0^+	299(2)	439
2^+	–	16.31
4^+	–	8.99
6^+	25(10)	26.99
8^+	490(150)	277
10^+	–	1.99×10^3
12^+	–	3.46×10^3
14^+	–	2.26×10^5
16^+	–	–
18^+	4.5×10^{10}	4.83×10^{10}

Table 4. The level scheme and electromagnetic transition strengths of ^{20}Ne. The parameter set is given by Eq. (11) with a new value of R=3.25 fm. The experimental values are taken from Refs. [38, 39]. The values for B(E2↓) are in the unit of the so-called Weisskopf unit (W.u.) given by 1 W.u. $=\frac{0.746}{4\pi}A^{4/3}$ e^2·fm^4. Here, $A=A_{\alpha}+A_c=20$ is the mass number of ^{20}Ne, and e is the elementary charge.

J^{π}	$E^{\rm exp}$/MeV	$E^{\rm present}$/MeV	B(E2↓)$_{\rm exp}$/(W.u.)	B(E2↓)$_{\rm present}$/(W.u.)
0^+	0.000	1.117	–	–
2^+	1.634	2.238	20.3±1.0	18.341
4^+	4.248	4.472	22.0±2.0	23.663
6^+	8.776	7.707	20.0±3.0	19.314
8^+	11.951	11.852	9.03±1.3	9.867

Table 5. The level scheme and electromagnetic transition strengths of ^{44}Ti. The parameter set is given by Eq. (11) with a new value of R=4.61 fm. The experimental values are taken from Refs. [9, 38]. Values for B(E2↓) are in the unit of the so-called Weisskopf unit (W.u.) given by 1 W.u. $=\frac{0.746}{4\pi}A^{4/3}$ e^2·fm^4. Here, $A=A_{\alpha}+A_c=44$ is the mass number of ^{44}Ti, and e is the elementary charge.

J^{π}	$E^{\rm exp}$/MeV	$E^{\rm present}$/MeV	B(E2↓)$_{\rm exp}$/(W.u.)	B(E2↓)$_{\rm present}$/(W.u.)
0^+	0.000	0.695	–	–
2^+	1.083	1.273	13.0±4.0	13.152
4^+	2.454	2.359	30.0±6.0	17.651
6^+	4.015	3.813	17.0±3.0	16.881
8^+	6.509	5.476	>1.52	13.752
10^+	7.671	7.152	14.97±3.0	9.307
12^+	8.039	8.555	<6.51	4.459

4 Conclusions

In summary, we investigated the alpha-cluster structures of various alpha + closed shell nuclei with a new phenomenological potential of the Woods-Saxon-Gaussian form, which modifies the original WS potential using an extra Gaussian form factor centered at the nuclear surface. With the parameter set given by Eq. (11), level schemes, reduced quadrupole transition strengths, and alpha-decay half-lives are found to be quite satisfying for ^{212}Po, and many important features of the experimental values are well-reproduced. This could be viewed as an explicit demonstration of the usefulness of the proposed WSG potential when applied to the study of nuclear clustering in heavy nuclei. Moreover, we provide some exploratory calculations in studying alpha-cluster structures in light nuclei using the WSG potential. Using the same parameter set Eq. (11), with the exception that new values are used for the radius R, we calculate the level schemes and electromagnetic transitions for ^{20}Ne and ^{44}Ti. These calculated values agree with the experimental results as well. The calculations reveal that the WSG potential proposed in this work is indeed a new phenomenological potential that is suitable for studying various properties of nuclear alpha-cluster structures. In this work, we have identified the radius in the Gaussian form factor with that in the WS potential. Considering the phenomenological success of the WSG potential, it is natural to question the microscopic origin of this choice. It may be related to the alpha-cluster formation process taking place at the nuclear surface and is an important open question to be investigated in future works.

Appendix A

Momentum-space approach to double-folding potentials

The double-folding potential is given by

$$U(\boldsymbol{r})=\lambda\int\rho_c(\boldsymbol{r}_1)\rho_\alpha(\boldsymbol{r}_2)V_{\rm NN}(\boldsymbol{r}_{12}=\boldsymbol{r}+\boldsymbol{r}_2-\boldsymbol{r}_1){\rm d}\boldsymbol{r}_1{\rm d}\boldsymbol{r}_2, \quad \text{(A1)}$$

where λ is the renormalization factor. It is convenient to calculate double-folding potentials in the momentum space [37]. The Fourier transformations are normalized by:

$$\tilde{f}(\boldsymbol{k})=\int{\rm d}\boldsymbol{r}\exp(i\boldsymbol{k}\cdot\boldsymbol{r})f(\boldsymbol{r}), \quad \text{(A2)}$$

$$f(\boldsymbol{r})=\frac{1}{(2\pi)^3}\int{\rm d}\boldsymbol{k}\exp(-i\boldsymbol{k}\cdot\boldsymbol{r})\tilde{f}(\boldsymbol{k}), \quad \text{(A3)}$$

which gives: $\int{\rm d}\boldsymbol{r}\exp(i\boldsymbol{k}\boldsymbol{r})=(2\pi)^3\delta(\boldsymbol{k})$. The density functions of the core nucleus, the alpha cluster and the nucleon-nucleon interaction take the following forms, respectively,

$$\rho_c(r_1)=\frac{\rho_1}{1+\exp\left(\frac{r_1-c}{a}\right)}, \quad \text{(A4)}$$

$$\rho_\alpha(r_2)=\rho_2\exp(-\nu r_2^2), \quad \text{(A5)}$$

$$V_{\rm NN}(\boldsymbol{r}_{12})=V_1\frac{\exp(-\mu_1 r_{12})}{\mu_1 r_{12}}+V_2\frac{\exp(-\mu_2 r_{12})}{\mu_2 r_{12}}+J_{00}\delta(\boldsymbol{r}_{12}), \quad \text{(A6)}$$

with their Fourier transformations given by:

$$\tilde{\rho}_c(k)=4\pi\int_0^\infty{\rm d}r_1 r_1\frac{\sin kr_1}{k}\rho_c(r_1), \quad \text{(A7)}$$

$$\tilde{\rho}_\alpha(k)=\rho_2\pi^{3/2}\nu^{-3/2}\exp\left(-\frac{k^2}{4\nu}\right), \quad \text{(A8)}$$

$$\tilde{V}_{\rm NN}(k)=\frac{4\pi V_1}{\mu_1}\frac{1}{k^2+\mu_1^2}+\frac{4\pi V_2}{\mu_2}\frac{1}{k^2+\mu_2^2}+J_{00}. \quad \text{(A9)}$$

The double-folding potential could then be obtained by:

$$U(\boldsymbol{r})=\frac{1}{(2\pi)^3}\int{\rm d}\boldsymbol{k}\exp(-i\boldsymbol{k}\cdot\boldsymbol{r})\tilde{\rho}_c(k)\tilde{\rho}_\alpha(k)\tilde{V}_{\rm NN}(k) \quad \text{(A10)}$$

$$=\frac{2}{\pi}\int_0^\infty\int_0^\infty{\rm d}k{\rm d}r_1\frac{r_1}{r}\sin kr\sin kr_1\rho_c(r_1)\tilde{\rho}_\alpha(k)\tilde{V}_{\rm NN}(k). \quad \text{(A11)}$$

Compared with the definition of the double-folding potential Eq. (A1) which contains a six-dimensional integration, Eq. (A11) with only a two-dimensional integration is much easier to handle numerically. The parameter set used in this work is given by:

$$\begin{aligned}
&\rho_1=0.181855\ {\rm fm}^{-3}, \quad c=1.07A_c^{1/3}\ {\rm fm}, \quad a=0.54\ {\rm fm},\\
&\rho_2=0.4299\ {\rm fm}^{-3}, \quad \nu=0.7024\ {\rm fm}^{-2},\\
&V_1=7999\ {\rm MeV}, \quad V_2=-2134\ {\rm MeV},\\
&J_{00}=-276(1-0.005E_\alpha/A_\alpha)\ {\rm MeV\cdot fm}^3,\\
&\mu_1=4\ {\rm fm}^{-1}, \quad \mu_2=2.5\ {\rm fm}^{-1}, \quad \lambda=0.51,
\end{aligned} \quad \text{(A12)}$$

with A_α=4, A_c=208, and E_α being the alpha-decay energy.

References

1 L. R. Hafstad and E. Teller, Phys. Rev., **54**: 681 (1938)
2 A. Tohsaki, H. Horiuchi, P. Schuck and G. Röpke, Phys. Rev. Lett., **87**: 192501 (2001) [nucl-th/0110014]
3 D. Bai and Z. Ren, Phys. Rev. C, **97**: 054301 (2018), arXiv:1804.05992 [nucl-th]
4 B. Zhou et al, Phys. Rev. Lett., **110**: 262501 (2013), arXiv:1304.1244 [nucl-th]
5 G. Gamow, Z. Phys. **51**: 204 (1928)
6 R. Gurney, and E. Condon, Nature (London), **122**: 439 (1928)
7 B. Buck, A. C. Merchant, and S. M. Perez, Phys. Rev. Lett., **65**: 2975 (1990)
8 B. Buck, A. C. Merchant, and S. M. Perez, Phys. Rev. C, **45**: 2247 (1992)
9 B. Buck, A. C. Merchant, and S. M. Perez, Phys. Rev. C, **51**: 559 (1995)
10 B. Buck, J. C. Johnston, A. C. Merchant and S. M. Perez, Phys. Rev. C, **53**: 2841 (1996)
11 V. Y. Denisov and A. A. Khudenko, Phys. Rev. C, **80**: 034603 (2009) Erratum: [Phys. Rev. C, **82**: 059902 (2010)]
12 T. T. Ibrahim, S. M. Perez, and S. M. Wyngaardt, Phys. Rev. C, **82**: 034302 (2010)
13 D. S. Delion and A. Dumitrescu, Atom. Data Nucl. Data Tabl., **101**: 1 (2015)
14 V. Y. Denisov, O. I. Davidovskaya, and I. Y. Sedykh, Phys. Rev. C, **92**: 014602 (2015) arXiv:1506.08005 [nucl-th]
15 P. Mohr, Eur. Phys. J. A, **53**: 209 (2017) arXiv:1710.02790 [nucl-th]
16 D. S. Delion, Z. Ren, A. Dumitrescu, and D. Ni, J. Phys. G, **45**: 053001 (2018)
17 M. Ismail and A. Adel, Phys. Rev. C, **97**: 044301 (2018)
18 C. Xu and Z. Ren, Nucl. Phys. A, **753**: 174 (2005)
19 D. Ni and Z. Ren, Nucl. Phys. A, **828**: 348 (2009)
20 D. Ni and Z. Ren, Nucl. Phys. A, **825**: 145 (2009)
21 D. Ni and Z. Ren, Phys. Rev. C, **80**: 014314 (2009)
22 D. Ni and Z. Ren, Phys. Rev. C, **80**: 051303 (2009)
23 D. Ni and Z. Ren, Phys. Rev. C, **81**: 024315 (2010)
24 D. Ni and Z. Ren, Phys. Rev. C, **82**: 024311 (2010)
25 K. Varga, R. G. Lovas, and R. J. Liotta, Phys. Rev. Lett., **69**: 37 (1992)
26 A. Astier, P. Petkov, M.-G. Porquet, D. S. Delion, and P. Schuck, Phys. Rev. Lett., **104**: 042701 (2010), arXiv: 0911.3502 [nucl-ex]
27 A. Astier, P. Petkov, M.-G. Porquet, D. S. Delion, and P. Schuck, Eur. Phys. J. A, **46**: 165 (2010), arXiv: 1004.1517 [nucl-ex]
28 D. S. Delion, R. J. Liotta, P. Schuck, A. Astier, and M. G. Porquet, Phys. Rev. C, **85**: 064306 (2012)
29 G. Röpke et al, Phys. Rev. C, **90**: 034304 (2014), arXiv: 1407.0510 [nucl-th]
30 C. Xu et al, Phys. Rev. C, **93**: 011306 (2016), arXiv:1511.07584 [nucl-th]
31 D. S. Delion, Theory of Particle and Cluster Emission (Springer-Verlag, Berlin, 2010)
32 S. M. Wang, J. C. Pei, and F. R. Xu, Phys. Rev. C, **87**: 014311 (2013)
33 K. Wildermuth and Y. C. Tang, A Unified Theory of the Nucleus, (Academic Press, New York, 1977)
34 E. Hiyama, Y. Kino, and M. Kamimura, Prog. Part. Nucl. Phys., **51**: 223 (2003)
35 S. A. Gurvitz and G. Kalbermann, Phys. Rev. Lett., **59**: 262 (1987)
36 S. A. Gurvitz, Phys. Rev. A, **38**: 1747 (1988)
37 G. R. Satchler and W. G. Love, Phys. Rept., **55**: 183 (1979)
38 National Nuclear Data Center (NNDC): https://www.nndc.bnl.gov
39 H. Abele and G. Staudt, Phys. Rev. C, **47**: 742 (1993)